

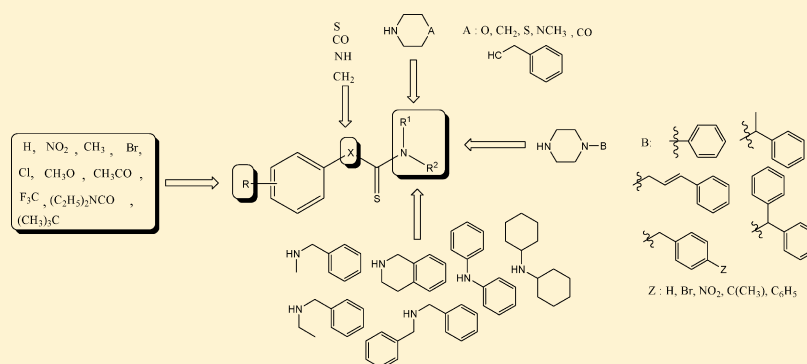
Synthesis and Pharmacological Evaluation of 2,4-Dinitroaryldithiocarbamate Derivatives as Novel Monoacylglycerol Lipase Inhibitors

Coco N. Kapanda,[†] Julien Masquelier,[‡] Geoffray Labar,[†] Giulio G. Muccioli,[‡] Jacques H. Poupaert,[†] and Didier M. Lambert^{*†}

[†]Medicinal Chemistry, Cannabinoid and Endocannabinoid Research Group, B1.73.10, Louvain Drug Research Institute (LDRI), Université Catholique de Louvain, 73 Avenue E. Mounier, B-1200 Bruxelles, Belgium

[‡]Bioanalysis and Pharmacology of Bioactive Lipids Research Group, B1.72.01, Louvain Drug Research Institute (LDRI), Université Catholique de Louvain, 72 Avenue E. Mounier, B-1200 Bruxelles, Belgium

Supporting Information



ABSTRACT: Monoacylglycerol lipase (MAGL) is responsible for signal termination of 2-arachidonoylglycerol (2-AG), an endocannabinoid neurotransmitter endowed with several physiological effects. Previously, we showed that the arylthioamide scaffold represents a privileged template for designing MAGL inhibitors. A series of 37 compounds resulting from pharmacomodulations around the arylthioamide template were synthesized and tested to evaluate their inhibitory potential on MAGL activity as well as their selectivity over fatty acid amide hydrolase (FAAH), another endocannabinoid-hydrolyzing enzyme. We have identified 2,4-dinitroaryldithiocarbamate derivatives as a novel class of MAGL inhibitors. Among the synthesized compounds, we identified [2,4-dinitrophenyl-4-(4-*tert*-butylbenzyl)piperazine-1-carbodithioate] (CK37), as the most potent MAGL inhibitor within this series ($IC_{50} = 154$ nM). We have also identified [2,4-dinitrophenyl-4-benzhydrylpiperazine-1-carbodithioate] (CK16) as a selective MAGL inhibitor. These compounds are irreversible MAGL inhibitors that probably act by interacting with Cys208 or Cys242 and Ser122 residues of the enzyme. Moreover, CK37 is able to raise 2-arachidonoylglycerol (2-AG) levels in intact cells.

INTRODUCTION

Monoacylglycerol lipase (MAGL) is one of the key enzymes of the endocannabinoid system (ECS). The ECS is implicated in several major physiological processes such as the regulation of pain, cognition, and cellular proliferation, both in the central nervous system and in peripheral organs. This signaling system consists of lipid messengers named endocannabinoids, along with synthesis and degradation enzymes as well as the G-protein-coupled CB₁ and CB₂ cannabinoid receptors that constitute their molecular targets.¹ Two endocannabinoids, 2-arachidonoylglycerol (2-AG) and *N*-arachidonylethanolamine (AEA), act as retrograde messengers for modulating synaptic transmission² and are the main endogenous ligands of CB₁ and CB₂ cannabinoid receptors.^{3–5} Unlike classical neurotransmitters, endocannabinoids are not stored in vesicles prior to their

release; they are produced on demand⁶ and are rapidly inactivated, following the activation of their targets, by cellular uptake and enzymatic hydrolysis.⁷ AEA is metabolized into arachidonic acid and ethanolamine by FAAH,^{8,9} and 2-AG is mainly hydrolyzed by MAGL. MAGL, a 33 kDa enzyme consisting of 303 amino acid residues, is a cytosolic serine hydrolase that is also found associated with the cell membrane. Alternatively, 2-AG is also hydrolyzed by ABHD6 and ABHD12 which account for approximately 4% and 9%, respectively, of brain 2-AG hydrolase activity.^{10–13} Inhibition of MAGL, which results in increased 2-AG levels, could present several beneficial therapeutic effects. For instance it was

Received: January 30, 2012

Published: May 31, 2012

recently reported that increasing endogenous 2-AG levels neutralizes colitis and related systemic inflammation.¹⁴ MAGL also regulates a fatty acid network that promotes cancer pathogenesis.^{15,16}

Taken together, these data suggest that MAGL is a potential target for the development of new drugs. Despite the elucidation of MAGL 3D structure,^{17,18} only a few MAGL inhibitors are described to date.^{19,20} These include disulfiram²¹ and its analogues, i.e., bis(dialkylaminethiocarbonyl)disulfide derivatives,²² the 1,3,4-oxadiazol-2(3H)-one, CAY10499,²³ and the carbamate JZL184,²⁴ which is one of the potent MAGL inhibitors known so far (Figure 1).

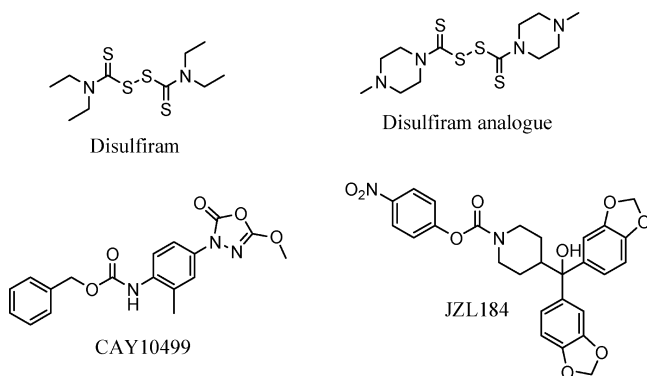


Figure 1. Structures of MAGL inhibitors.

Given the physiological role of this enzyme, the search for new inhibitors, belonging to new chemical families and endowed with original mechanisms of action, is of the utmost importance.

We report herein the synthesis and pharmacological evaluation of 2,4-dinitroaryldithiocarbamate derivatives as original MAGL inhibitors. These compounds are derived from chemical modifications of the arylthioamide scaffold. Indeed, in our previous report, we have described arylthioamide scaffold as a useful template for designing potent and selective MAGL inhibitors.²⁵ Hence, we have undertaken chemical modifications around arylthioamide scaffold in order to increase the potency and selectivity for MAGL inhibition as well as to establish the SAR of these new inhibitors. As potent MAGL

inhibitors, such as JZL184²⁴ and triazolopyridine or triazolopyrimidine carboxamide¹⁸ derivatives, have been reported to interact optimally with the acyl-binding pocket through a sterically hindered lipophilic moiety, we have developed a series of compounds based on the benzhydrylpiperazine template. We have studied the effects related to the modification of the lipophilicity, the influence of electronic effect, and conformational freedom. Moreover, we have evaluated the role of hydrogen bond acceptors for MAGL inhibition. Finally, using our lead compound, we have explored the mode of inhibition of MAGL as well as the ability of these inhibitors to modulate 2-AG levels in intact cells.

RESULTS AND DISCUSSION

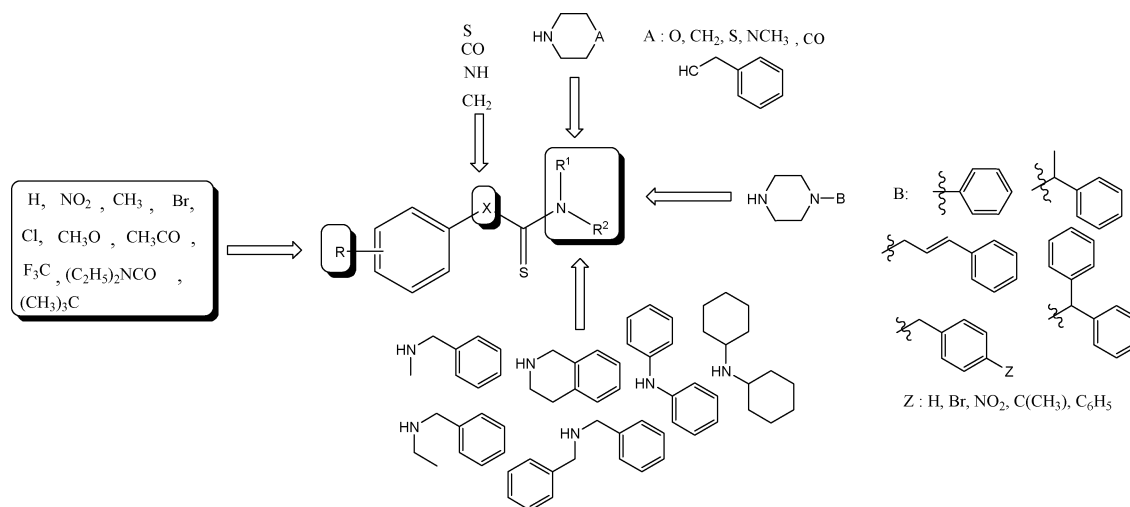
Chemistry. We previously reported that the arylthioamide template ($X = \text{CH}_2$, Scheme 1), in contrast to the arylamide one, could represent a useful scaffold for designing new MAGL inhibitors.²⁵ Thus, pharmacomodulations around the arylthioamide scaffold were undertaken while keeping constant aryl and thiocarbonyl moieties in all structures (see Scheme 1).

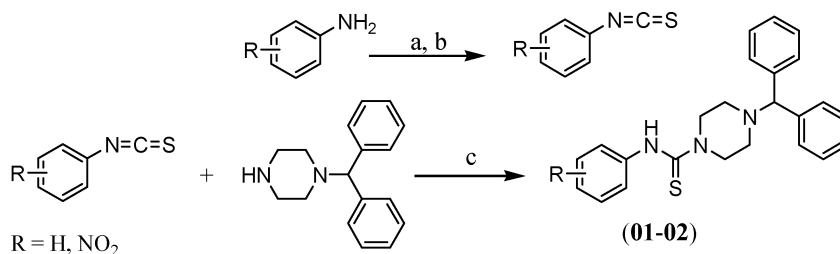
For this purpose, we modified the substituents on the aryl ring and used several secondary amines. Furthermore, the methylene link between the aryl and the thiocarbonyl of arylthioamide scaffold ($X = \text{CH}_2$, Scheme 1) was substituted successively by sulfur, nitrogen, or carbonyl. These pharmacomodulations led to the synthesis of arylthiourea ($X = \text{NH}$, **01** and **02**), aryloxothioamide ($X = \text{CO}$, **03** and **04**), and aryldithiocarbamate ($X = \text{S}$, **05–37**) derivatives as illustrated in the Scheme 1.

The target arylthiourea derivatives ($X = \text{NH}$, Scheme 1) **01** and **02** were obtained by reacting phenyl isothiocyanate or 4-nitrophenyl isothiocyanate with 1-benzhydrylpiperazine in methyl alcohol at room temperature (yield, 70–80%). We synthesized the aryl isothiocyanate by a two-step reaction. Aniline or 4-nitroaniline reacts with carbon disulfide in triethylamine to give a dithiocarbamate intermediate which upon treatment with di-*tert*-butyl dicarbonate (Boc_2O) and 1,4-diazabicyclo[2.2.2]octane (DABCO) yields the desired phenyl isothiocyanate derivative²⁶ (Scheme 2).

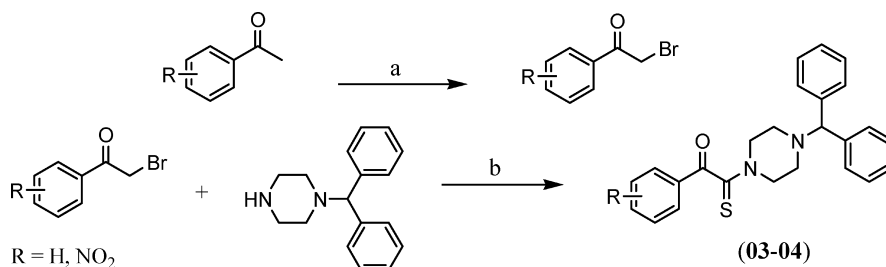
For the aryloxothioamide derivatives ($X = \text{CO}$, Scheme 1), the target compounds **03** and **04** were obtained in a one-pot reaction, with fairly good yields, by reacting the 2-bromo-1-

Scheme 1. Pharmacomodulations around the Arylthioamide Scaffold



Scheme 2. Syntheses of the Phenyl Isothiocyanate Derivatives and of the Target Phenylthiourea Derivatives 01 and 02^a

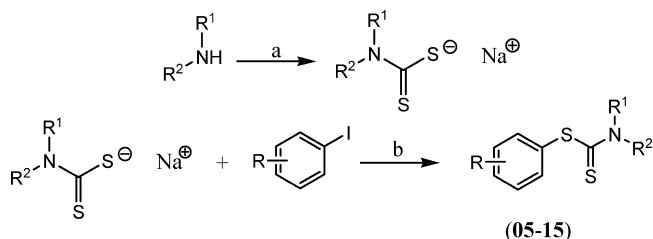
^aReagents and conditions : (a) triethylamine, CS₂, rt, 30 min; (b) Boc₂O, DABCO, 5 °C to rt, 20 min (61–93%); (c) methanol, rt, 30 min (80–90%).

Scheme 3. Syntheses of 2-Bromo-1-phenylethanone Derivatives and of the Target Aryloxothioamide Derivatives 03 and 04^a

^aReagents and conditions : (a) Br₂, CHCl₃, rt, 12 h (60–70%); (b) S₈, DMF, rt, 12 h (30–50%).

phenylethanone with sulfur and 1-benzhydrylpiperazine at room temperature, following a protocol adapted from Asinger et al.²⁷ The 2-bromo-1-phenylethanone derivative was obtained by brominating acetophenone in chloroform²⁸ (Scheme 3).

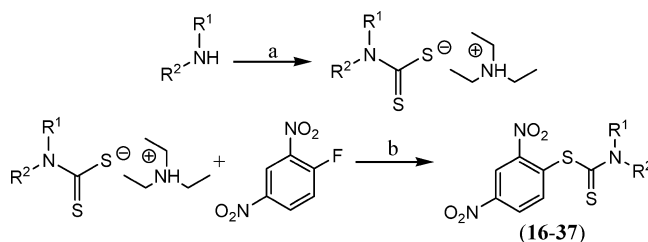
The Ullman-type coupling reaction was used to synthesize dithiocarbamate derivatives (X = S, Scheme 1) (05–15, Scheme 4). Thus, a substituted iodobenzene and dithiocarba-

Scheme 4. Syntheses of Dithiocarbamic Acid Sodium Salt and of the Dithiocarbamate Derivatives (05–15) through Ullman-Type Reaction^a

^aReagents and conditions: (a) NaOH aq, CS₂, rt, 3 h (90–98%); (b) CuI, *N,N*-dimethylglycine, DMF, 110 °C, 22 h (55–90%).

mic acid sodium salt were reacted in anhydrous DMF in the presence of copper(I) iodide and *N,N*-dimethylglycine for 22 h at 110 °C.²⁹ Beforehand, dithiocarbamic acid salts were obtained by reacting the desired amine with carbon disulfide in triethylamine or in aqueous sodium hydroxide solution³⁰ (Scheme 4).

Finally, the 2,4-dinitroaryldithiocarbamate derivatives 16–37 were obtained by reaction of a dithiocarbamic acid salt with 2,4-dinitrofluorobenzene using the well-known Sanger reaction (Scheme 5). The dithiocarbamic acid salts were prepared by reacting the appropriate secondary amine with CS₂ in the presence of triethylamine as shown in Scheme 5.

Scheme 5. Syntheses of Dithiocarbamic Acid Triethylammonium Salt and of the Dithiocarbamate Derivatives 16–37 through Sanger-Type Reaction^a

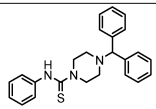
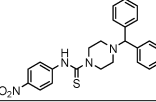
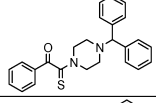
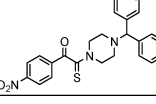
^aReagents and conditions: (a) triethylamine, CS₂, rt, 3 h (90–98%); (b) DMF, rt, 12 h (80–95%).

Note that the benzhydrylpiperazine derivatives not commercially available, i.e., 1-(4-bromobenzyl)piperazine, 1-(4-phenylbenzyl)piperazine, and 1-(4-*tert*-butylbenzyl)piperazine, were prepared from conveniently substituted 1-(bromomethyl)benzene reacting with piperazine in THF.³¹

Pharmacological Evaluation. We have, first, evaluated the inhibitory potential of synthesized compounds by determining their pIC₅₀ values (i.e., $-\log IC_{50}$ (M)) for human MAGL and FAAH inhibition. Subsequently, the mechanism of inhibition was studied by evaluating the reversibility of the inhibition, as well as the potential formation of disulfide bonds between the inhibitors and MAGL. Finally we determined whether these compounds are indeed able to increase 2-AG levels by inhibiting MAGL in intact cells.

1. Evaluation of Inhibitory Potential: Determination of pIC₅₀. We have determined the inhibitory potential of the synthesized compounds by performing a dose-dependent activity assay on two major enzymes of the ECS (i.e., MAGL and FAAH), using human recombinant MAGL and FAAH developed in our laboratory. Thus, hydrolysis of tritiated 2-oleoylglycerol ([³H]-2-OG) by purified human MAGL was

Table 1. Influence of the Dithiocarbamate Moiety on the Inhibition of hMAGL and hFAAH

Cpds	Structure	pIC ₅₀		Selectivity ratio
		MAGL	FAAH	
01		<3	<3	ND
02		4.53±0.05	<3	> 34
03		<3	<3	ND
04		4.66±0.09	<3	> 46

used to evaluate the ability of our compounds to inhibit MAGL esterase activity.²¹ Similarly, the FAAH assay consisted of the measurement of tritiated *N*-arachidonylethanolamine ([³H]-AEA) hydrolysis by human FAAH.³² The obtained results are presented in Tables 1–3.

Among the compounds presented in Tables 1 and 2, 4-nitroaryldithiocarbamate derivatives exhibit both higher activity and selectivity (compound **15**) compared with arylthiourea (**02**) and aryloxothioamide (**04**) derivatives. The higher MAGL inhibition obtained with the arylthiocarbamate could be explained, on the one hand, by the high versatility of divalent sulfur atom, which is characterized by its ability to interact with both electron-poor and electron-rich functional groups.³³ The electron-rich ones tend to approach divalent sulfur along the extension of the C–S bond (σ^* direction). On the other hand, unlike in the case of arylthiourea (**02**) and aryloxothioamide (**04**) derivatives, the presence of 4-nitrothiophenolate as a leaving group contributes significantly to the inhibitory potency of compound (**15**). To further confirm this hypothesis and to enhance MAGL inhibitory activity of these derivatives, we have synthesized compounds bearing a 2,4-dinitroaryl moiety in which 2,4-dinitrophenolate constitutes an excellent leaving group. By using several amines, we have highlighted the importance of 1-benzhydrylpiperazine in MAGL inhibition also within this series of inhibitors (Table 3).

As shown in Tables 2 and 3 (**15** vs **16**), two nitro groups are necessary to obtain higher MAGL inhibitory activity within the arylthiocarbamate series.

The MAGL inhibition appears to be related mainly to the reactivity, molecular size, and lipophilicity. Regarding the reactivity, high MAGL inhibition is obtained with compounds bearing an activated leaving group (aromatic ring substituted with one (**15**) or two (**16**) nitro groups). We can thus hypothesize, taking into account the low MAGL inhibitory activity of compounds (**05**–**14**) as well as the activity of compound (**15**), that the withdrawing electronic effect of nitro groups makes the thiocarbonyl group sensitive to nucleophilic attack, i.e., able to react with serine and/or cysteine residues of MAGL. Indeed, it is well established that carbamate-based MAGL inhibitors interact with the nucleophilic serine (Ser122) of MAGL through the electrophilic carbonyl²⁴ and that isothiazolinone or disulfide-based compounds inhibit MAGL by reacting with the cysteine residues (Cys208/242).^{22,34}

In contrast to carbamate derivatives that required a six-member ring (*N*-piperidine/piperazine group) to maintain activity,³⁵ cyclic amine is not required for MAGL inhibition within this series, as demonstrated by the MAGL inhibition obtained with derivatives **24**–**27** and **29**.

During exploration of the nature of the substituent with various small amines bearing either a hydrogen bond acceptor moiety (compounds **18**, **19**, and **21**) or not (compounds **20**, **22**–**23**), the inhibitory activity on MAGL remains unchanged. This is consistent with our structural knowledge of the MAGL active site. On the one hand, the wide active site of the enzyme allows the accommodation of a vast range of substituents, but on the other hand, it is likely less well adapted to the formation of contributive interactions between small amines of compounds **17**–**28** and MAGL residues.

Besides this, a more voluminous substituent, when carefully selected as in the case of compounds **16** and **37**, allows a substantial gain in activity compared to derivatives bearing a *N*-methylpiperazine (**17**), morpholine (**18**), or thiomorpholine (**21**) moiety.

Regarding FAAH, the narrower active site of the enzyme, reported in several crystal structures, likely explains the loss of FAAH affinity and gain in MAGL selectivity displayed by bulkier inhibitors like **24**, **25**, and **16**.

Interestingly, rigidification of compound **27**, a nonselective MAGL and FAAH inhibitor, led to the 1 order of magnitude more selective compound **28**, which showed a significant decrease of inhibitory potency for FAAH. Again, this could reflect the more stringent conditions, in terms of steric hindrance, required to fit into the FAAH active site. The higher intrinsic conformational freedom of compound **27**, compared to **28**, could allow it to fit more easily into the FAAH active site.

We found that the methylene link between the piperazine moiety and the phenyl ring is important for MAGL inhibition. In fact, **30**, which does not possess a methylene link, and its analogue **31** bearing this link, have pIC₅₀ values of 5.11 and 6.00, respectively. Increasing the length of the methylene linker (**33**) or its methylation (**34**) does not improve the inhibitory activity against MAGL. Adding a phenyl group at the para-position in **31**, resulting in derivative **35**, slightly decreased both activity and selectivity, while a *tert*-butyl group in the same position (**37**) led to the most potent compound within this series (pIC₅₀ = 6.81). With 4-bromobenzyl as substituent (**36**),

Table 2. Influence of Phenyl Ring Substitution on the Inhibition of hMAGL and hFAAH

Cpds	Structure	pIC ₅₀		Selectivity ratio
		MAGL	FAAH	
05		<3	<3	ND
06		<3	<3	ND
07		<3	<3	ND
08		<3	<3	ND
09		4.02±0.05	<3	<10
10		<3	<3	ND
11		<3	<3	ND
12		4.16±0.09	<3	<10
13		<3	<3	ND
14		<3	<3	ND
15		5.13±0.03	<3	> 135

the activity, but not the selectivity, is increased when compared to **31**. Thus, we have identified **16** and **37** as highly active MAGL inhibitors, with **16** showing a high selectivity for MAGL compared to FAAH inhibition.

II. Investigations of the Inhibition Mechanism. II.1. Evaluation of the Inhibition Reversibility. Rapid dilution assays were performed in order to evaluate the reversibility of the inhibition. For this purpose, according to a well established method,^{23,36} **37** was incubated with MAGL solution at four different concentrations, 10^{-3} , 10^{-4} , 10^{-5} , and 10^{-6} M, followed by a 300 times dilution prior to assaying MAGL activity. Thus, after dilution, the concentrations should correspond to $10^{-5.5}$, $10^{-6.5}$, $10^{-7.5}$, and $10^{-8.5}$ M, respectively. The strong MAGL inhibition still observed following the 10^{-6} M \rightarrow $10^{-8.5}$ M dilution, while no inhibition is present when MAGL is directly incubated with $10^{-8.5}$ M **37** (Figure 2), suggests the establishment of a covalent bond between the enzyme and

the inhibitor, thereby providing strong evidence for irreversible mechanism of inhibition.

II.2. Investigation of the Formation of Disulfide Bonds between **37 and MAGL.** To further investigate the inhibition mechanism, the potential formation of a disulfide bond between **37** and the enzyme was evaluated using dithiothreitol (DTT), a disulfide bond reducing agent. Therefore, **37** was preincubated with MAGL (room temperature, 30 min) prior to DTT addition. The concentrations of **37** ($10^{-4.5}$ and 10^{-5} M) were chosen to fully inhibit MAGL activity. After DTT addition, the mixture was incubated at room temperature for an additional 15 min to allow for DTT reaction, after which MAGL activity was assessed using the usual protocol.

We found that MAGL activity was restored to a large extent following DTT incubation (Figure 3). This suggests the formation of a disulfide bond as part of the inhibition mechanism. However, one cannot exclude the formation of

Table 3. Influence of the Structure of the 2,4-Dinitroaryl Moiety and of the Amine on the Inhibition of hMAGL and hFAAH^a

Cpds	Structure	pIC ₅₀		Selectivity ratio
		MAGL	FAAH	
16 (CK16)		6.45±0.08	<3	2818
17		5.75±0.05	4.63±0.06	13
18		5.37±0.05	4.27±0.08	13
19		5.29±0.02	4.01±0.07	12
20		5.62±0.12	4.33±0.02	19
21		5.43±0.08	4.72±0.14	13
22		5.22±0.08	4.35±0.10	7
23		5.52±0.12	4.65±0.04	7
24		5.58±0.09	<3	>380
25		5.70±0.07	<3	>501
26		5.66±0.09	6.03±0.06	0.4
27		5.27±0.04	5.28±0.08	0.9
28		5.15±0.08	4.28±0.03	7
29		5.30±0.06	5.17±0.10	1.3
30		5.11±0.09	5.56±0.08	0.3
31		6.00±0.02	4.73±0.12	19
32		6.08±0.05	5.70±0.02	2
33		6.01±0.06	5.31±0.09	5
34		6.09±0.04	4.80±0.08	20
35		5.75±0.08	5.59±0.07	1.4
36		6.36±0.05	5.94±0.09	3
37 (CK37)		6.81±0.06	5.76±0.05	11

^aValues are the mean ± standard error of the mean (SEM) from three independent experiments performed in duplicate.

an adduct between **37** and the catalytic serine as MAGL activity was not completely restored following DTT incubation.

To identify the cysteine residue(s) implicated in the inhibition process, we used total homogenates of *E. coli* expressing mutated hMAGL constructs, i.e., C201A, C208A,

C242A, and C208A/C242A. According to our results, Cys201 is not implicated in the inhibition mechanism (Figure 4). In fact, the C201A mutation does not affect the MAGL inhibition by **37** when compared to the inhibition observed with wild-type (WT) MAGL. However, there is a significant implication of

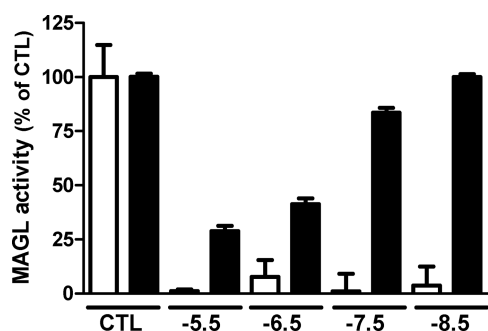


Figure 2. Reversibility of MAGL inhibition by 37. MAGL activity was tested following 30 min of incubation of the enzyme in the presence of four concentrations of 37 followed by a 300× dilution of the protein–inhibitor mixture (white histogram). The same concentrations were also assayed using the usual protocol (black histogram). The difference demonstrates the irreversible nature of the inhibition. Data are expressed as percent of the respective controls: (***) $P < 0.001$ compared to CTL (one-way ANOVA, Dunnett's post hoc test).

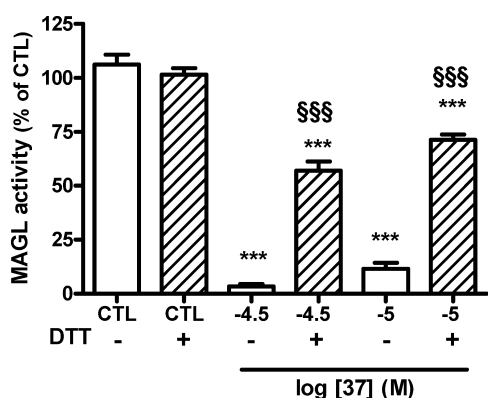


Figure 3. Influence of DTT on MAGL inhibition by 37. MAGL and compound 37 (at $10^{-4.5}$ and 10^{-5} M) were incubated for 30 min, and then DTT or vehicle was added to the mixture and incubated for 15 min. MAGL activity was then assessed as described. MAGL activity was normalized to the respective control. Of note, DTT had no effect on the basal activity of MAGL, i.e., CTL vs CTL + DTT: (***) $P < 0.001$ compared to the respective control; (§§§) $P < 0.001$ compared to the same condition without DTT (one-way ANOVA, Bonferroni's post hoc test).

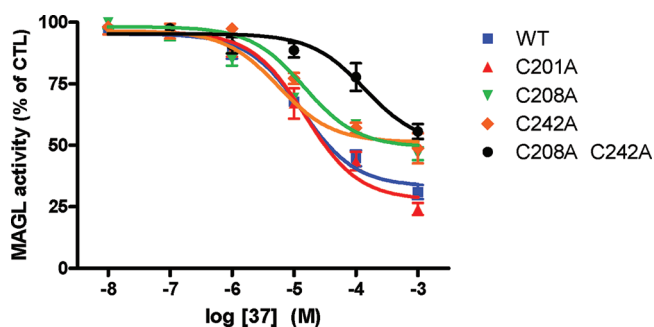


Figure 4. Inhibition of wild-type and mutated MAGL by 37. The inhibitor was assayed ($n = 3$, in duplicate) using homogenates of *E. coli* expressing either the wild-type MAGL (WT) or C201A, C208A, C242A, and C208A/C242A mutated enzymes. Note that 37 appears less potent against WT MAGL (compared to its IC_{50} reported in Table 3) because of the use of *E. coli* total homogenate for this figure rather than of purified MAGL (as for Table 3).

Cys208 and Cys242 in the inhibition process. Indeed 37 is less efficacious in inhibiting C208A and C242A MAGL mutants compared to the WT-MAGL, as can be deduced by the higher residual activity of the mutated enzymes. When both mutations are combined (MAGL C208A/C242A), the inhibitor is less efficacious, but also less potent, when compared to its inhibitory activity on WT MAGL. These elements point to two cysteine residues, Cys208 and Cys242, as key residues in the interaction between this class of inhibitors and MAGL. In all three MAGL crystal structures reported to date, Cys208 is located on the outside surface of the enzyme, 18 Å away from the catalytic serine, and it points toward the outside of the active site. It is thus not clear how a covalent modification of this residue could lead to an inhibition of the enzyme except if we assume that an allosteric inhibition occurs following the binding of compound 37. In contrast, Cys242 is located at the center of the active site, at 5 Å of the nucleophilic serine hydroxyl group.

Interestingly, as was observed when DTT was used to reverse the inhibition (see Figure 4), 37 is still able to interact with the double mutant C208A/C242A, suggesting that it might also interact with other residues such as the catalytic serine.

III. Activity of Compounds 16 and 37 on MAGL Inhibition in an Intact, Mammalian, Cellular System. Having tested these novel inhibitors in vitro on purified hMAGL, we next wanted to assess whether our most active (37) and selective (16) inhibitors would be able to interact with MAGL in an intact cellular system. Thus, we used a murine melanoma cell line endogenously expressing MAGL as a model and evaluated the ability of the inhibitors to enter the cell and to interact with MAGL by measuring the levels of endogenously produced 2-AG. Following an 8 h incubation of the cells in the presence of inhibitor, 37 was able to induce a significant increase in 2-AG levels (Figure 5).³⁷

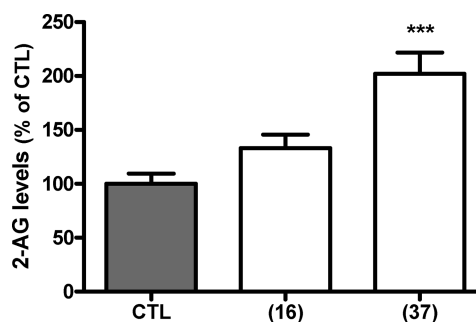


Figure 5. Influence of 16 and 37 on the cellular levels of 2-AG. B16 melanoma cells were incubated 8 h in the presence of either 0.1% DMSO (CTL) or 10 μM 16 or 37. After the incubation, the medium and the cells were recovered and the levels of 2-AG quantified by an isotope-dilution HPLC–MS method using d_5 -2-AG as internal standard.³⁷

Of interest, despite a comparable structure, ClogP, and affinity for the enzyme, 16 only slightly increased 2-AG levels in contrast to the robust increase observed with 37. The observed difference in the 2-AG levels after MAGL inhibition could be explained by differences in the metabolic fate or/and differences of their stability in the cellular media. Note that although FAAH is expressed by these cells, the well-known FAAH inhibitor URB-597, used in the same conditions, does not increase 2-AG levels while increasing *N*-acylethanolamine

levels (data not shown), thus ruling out the involvement of FAAH in the effect of **37** on 2-AG levels.

CONCLUSIONS

Starting from a modest arylthioamide hit,²⁵ we have developed a novel series of arylthiocarbamate inhibitors of MAGL. The activity of these inhibitors is highly dependent on the presence of 2,4-dinitrophenolate as a leaving group, suggesting that the inhibitors react with their enzymatic target. Indeed, we demonstrate here that these inhibitors irreversibly inhibit MAGL via formation of a DTT-sensitive covalent bond with either Cys208 or Cys242, two noncatalytic cysteine residues, and/or the catalytic Ser122 of the MAGL. By structure–activity relationships studies we have identified 2,4-dinitrophenyl 4-(4-*tert*-butylbenzyl)piperazine-1-carbodithioate (**37**) as a potent and quite selective MAGL inhibitor. We have also identified 2,4-dinitrophenyl 4-benzhydrylpiperazine-1-carbodithioate (**16**) as a submicromolar and highly selective MAGL inhibitor. The efficacy in inhibiting pure hMAGL *in vitro*, coupled to its ability to increase cellular levels of 2-AG in intact cells, makes **37** a promising MAGL inhibitor, which should prove to be useful for future investigation of endocannabinoid degradation pathways.

EXPERIMENTAL SECTION

Chemistry. General Procedures. All reagents and solvents of analytical grade purchased from commercial sources (Sigma-Aldrich and Acros Organics) were used without further purification. The structures of all compounds synthesized were consistent with their NMR spectra and high resolution mass spectra. Melting points were determined in open capillaries using the Electrothermal 9100 apparatus and are reported uncorrected. Nuclear magnetic resonance (¹H and ¹³C) spectra were recorded on a Bruker Avance 400 MHz Ultrashield instrument. Chemical shifts (δ) are reported relative to the tetramethylsilane peak set at 0 ppm. In the case of multiplets, the signals are reported as intervals. Signals are abbreviated as follows: s, singlet; d, doublet; t, triplet; q, quartet; qt, quintet; m, multiplet. Coupling constants are expressed in hertz. HRMS data for all final compounds were obtained using a LTQ-Orbitrap mass spectrometer (Thermo-Fisher Scientific) with the analysis performed using an ESI source in both positive and negative modes. All tested compounds were at least 95% pure as determined using an Accela HPLC system (Thermo-Fisher Scientific). Separation was performed using a RP-18 column (3 μ M, 4 mm \times 150 mm; Sigma-Aldrich).

Thiourea Derivatives Synthesis (01 and 02). To a solution of aryl isothiocyanate (see Supporting Information, p S2) in methanol (0.01 mol) was added 1-benzhydrylpiperazine (0.012 mol). The mixture was stirred for 3 h at room temperature and the reaction monitored by TLC. After completion of the reaction, the precipitate was filtered off and purified by column chromatography (ethyl acetate/hexane, 2:8) to yield the target product (80–90%).

4-Benzhydryl-*N*-phenylpiperazine-1-carbothioamide (01). Mp 215–217 °C. ¹H NMR (DMSO-*d*₆): δ (ppm) 9.29 (s, 1H), 7.48–7.10 (m, 15H), 4.38 (s, 1H), 3.93 (t, 4H, *J* = 4.88 Hz), 2.38 (t, 4H, *J* = 4.88 Hz). ¹³C NMR (DMSO-*d*₆): δ (ppm) 181.29, 142.34, 140.97, 133.05, 128.58, 127.98, 127.65, 126.99, 125.17, 124.24, 74.47, 51.20, 47.97. HRMS: [M + H]⁺ = 388.183 24.

The details for compound **02** can be found in the Supporting Information (p S3).

Aryloxothioamide Derivatives Synthesis (03 and 04). The used protocol was adapted from Asinger et al.²⁹ To a suspension of 2-bromo-1-phenylethanone (see Supporting Information, p S2) (0.1 mol) and sulfur (19.2 g) in DMF (50 mL) was added 1-benzhydrylpiperazine (0.35 mol). The reaction mixture was stirred overnight at room temperature. The mixture was then poured into water, and the crude product was extracted with dichloromethane. The organic phase was dried on sodium sulfate and then, concentrated under reduced pressure. Purification on silica gel column using ethyl

acetate/hexane, 5:5 (v/v), as eluent afforded the pure product (30–50%).

2-(4-Benzhydrylpiperazin-1-yl)-1-phenyl-2-thioxoethanone (03). Mp 125–127 °C. ¹H NMR (CDCl₃): δ (ppm) 7.89–7.22 (m, 15H), 4.22 (s, 1H) 3.51 (t, 2H, *J* = 4.84 Hz), 3.49 (t, 2H, *J* = 4.76 Hz), 2.56 (t, 2H, *J* = 4.84 Hz), 2.35 (t, 2H, *J* = 4.76 Hz). ¹³C NMR (CDCl₃): δ (ppm) 195.05, 188.00, 141.60, 134.27, 133.34, 129.83, 128.89, 128.78, 127.75, 127.44, 75.58, 51.75, 51.68, 51.12, 46.99. HRMS: [M + H]⁺ = 401.166 81.

The details for compound **04** can be found in the Supporting Information (p S3).

Dithiocarbamate Derivatives Synthesis. Dithiocarbamates derivatives **05–15** were obtained by a Ullman-type coupling reaction.

To a solution of *N,N*-dimethylglycine (30 mol %), dithiocarbamic acid sodium salt (1.2 mmol), obtained as reported by Sattigeri et al.,³⁰ and substituted aryl iodide (1 mmol) in anhydrous DMF (2 mL) was added CuI (15 mol %). Under nitrogen atmosphere, the mixture was stirred at 110 °C for 22 h. The reaction mixture was then cooled to room temperature, poured in water and extracted with ethyl acetate. The combined organic layer was dried over magnesium sulfate. After evaporation of ethyl acetate, the product was purified by column chromatography (petroleum ether/ethyl ether, v/v = 4/1) (55–90%).

Phenyl 4-Benzhydrylpiperazine-1-carbodithioate (05). Mp 157–159 °C. ¹H NMR (CDCl₃): δ (ppm) 7.44–7.19 (m, 15H), 4.29 (s, 1H), 4.29 (t, 2H, *J* = 3.28 Hz), 4.04 (t, 2H, *J* = 3.92 Hz), 2.54 (m, 4H). ¹³C NMR (CDCl₃): δ (ppm) 197.09, 141.87, 137.10, 131.28, 130.07, 129.83, 129.10, 128.73, 127.86, 127.34, 75.71, 51.40, 48.8. HRMS: [M + H]⁺ = 405.144 17.

The details for compounds **06–15** can be found in the Supporting Information (pp S3–S5).

Nucleophilic Aromatic Substitution (16–37). The target arylthiocarbamates **16–37** were obtained by a nucleophilic aromatic substitution using the following protocol. To a solution of dithiocarbamic acid triethylammonium salt (see Supporting Information, p S2) (1.2 mmol) in *N,N*-dimethylformamide (5 mL) was added 2,4-dinitrofluorobenzene (1 mmol). The mixture was stirred overnight at room temperature, dissolved in water, and extracted with dichloromethane. The organic phase was dried over sodium sulfate and evaporated under reduced pressure. Crystallization from ethanol afforded the pure product. In some cases further purification using column chromatography (silica gel, ethyl acetate/hexane, 3:7 v/v) was needed (80–95%).

2,4-Dinitrophenyl 4-Benzhydrylpiperazine-1-carbodithioate (16). Mp 157–159 °C. ¹H NMR (CDCl₃): 8.75 (d, 1H, *J* = 2.32 Hz), 8.32 (dd, 1H, *J* = 6.16 Hz), 7.78 (d, 1H, *J* = 8.64 Hz), 7.36–7.11 (m, 10H), 4.23 (s, 1H), 4.01 (t, 2H, *J* = 4.84 Hz), 3.99 (t, 2H, *J* = 4.84 Hz), 2.48 (t, 4H, *J* = 4.84 Hz). ¹³C NMR (CDCl₃): δ (ppm) 189.90, 151.20, 147.90, 141.67, 139.35, 135.14, 128.81, 127.82, 127.47, 126.19, 120.44, 75.56, 52.16, 51.94, 51.64, 51.23. HRMS: [M + H]⁺ = 495.113 34.

2,4-Dinitrophenyl 4-(4-*tert*-Butylbenzyl) piperazine-1-carbodithioate (37). Mp 128–130 °C. ¹H NMR (CDCl₃): δ (ppm) 8.85 (d, 1H, *J* = 2.32 Hz), 8.43 (dd, 1H, *J* = 6.32 Hz), 7.89 (d, 1H, *J* = 8.60 Hz), 7.37–7.23 (m, 4H), 4.34 (t, 2H, *J* = 4.36 Hz), 4.06 (t, 2H, *J* = 4.52 Hz), 3.52 (s, 1H), 2.61 (t, 2H, *J* = 4.36 Hz), 2.57 (t, 2H, *J* = 4.52 Hz), 1.35 (s, 9H). ¹³C NMR (CDCl₃): δ (ppm) 190.01, 151.31, 150.53, 147.95, 139.46, 135.07, 134.05, 128.87, 126.45, 125.38, 120.43, 62.01, 52.59, 52.28, 51.90, 34.54, 31.39. HRMS: [M + H]⁺ = 475.144 97.

The details for compounds **17–36** can be found in the Supporting Information (pp S6–S10).

Pharmacological Evaluation. MAGL Esterase Activity Assay. Measurement of radiolabeled 2-oleoylglycerol (2-OG) hydrolysis by MAGL was performed as previously described.²¹ Briefly, 2-OG (10 μ M, [³H]-2-OG, 50 000 dpm, American Radiolabeled Chemicals) was incubated at 37 °C for 10 min in the presence of purified recombinant hMGL (5 ng in Tris buffer, pH 8.0, 50 mM, 0.1% BSA, 200 μ L of total volume assay) and 10 μ L of DMSO (controls) or inhibitors (dissolved in DMSO). The incubation was stopped by adding 400 μ L of an ice-cold 1:1 methanol–chloroform mixture to each tube and thorough mixing. After centrifugation at 700g for 5 min, radioactivity in the

upper aqueous layer was measured by liquid scintillation. Blanks (i.e., tubes containing no enzyme) were made for each experiment (and the values subtracted from all the other values). Results are reported as pIC_{50} ($pIC_{50} = -\log IC_{50}$ (M)). GraphPad Prism was used to treat data.

FAAH Activity Assay. FAAH (6 ng of proteins/tube in 175 μ L of Tris-EDTA buffer) was added to glass tubes containing the drugs dissolved in DMSO, or DMSO alone (10 μ L). Hydrolysis was initiated by adding 25 μ L of [3 H]anandamide ([3 H]AEA, 50 000 dpm, American Radiolabeled Chemicals, 2 μ M final concentration) and by incubating the glass tubes at 37 $^{\circ}$ C. After incubation (10 min), the reaction was stopped by rapidly adding 400 μ L of ice-cold methanol–chloroform (1:1 v/v). Following centrifugation (850g, 5 min, 4 $^{\circ}$ C) the [3 H]ethanolamine in the aqueous layer was recovered and counted by liquid scintillation. Blanks were prepared (buffer instead of FAAH) and the values systematically subtracted. Results are reported as pIC_{50} ($pIC_{50} = -\log IC_{50}$). GraphPad Prism was used to treat data.

Evaluation of the Inhibition Reversibility by Using Rapid and High Dilution Assay. In a total volume of 20 μ L, pure MAGL (105 ng) was incubated during 30 min at room temperature with 1 μ L of 37 solution in DMSO (or DMSO alone, for controls). Immediately after, this enzyme–inhibitor mixture was diluted 300-fold by adding 6 mL of Tris buffer, pH 8.0. After 15 min of incubation, an aliquot (175 μ L) was taken and an amount of 25 μ L of substrate was added. The enzyme activity was then measured according to the above-described standard procedure.

Influence of 1, 4 Dithio-DL-threitol (DTT) on MAGL Inhibition by 37. The enzyme (3 ng in Tris buffer, pH 8.0, 50 mM, 0.1% BSA) was incubated for 10 min at room temperature in the presence of compound 37 at $10^{-4.5}$ and 10^{-5} M or of DMSO (control). DTT (10^{-2} M) was then added and the mixture incubated for 15 min (37 $^{\circ}$ C) prior to the substrate addition. The enzyme activity was measured according to the above-described standard procedure.

Influence of 16 and 37 on 2-AG Levels in Murine Melanoma B16 Cell Line. The murine melanoma cell line B16 (kindly donated by O. Feron, Université Catholique de Louvain, Belgium) was routinely cultured in minimum essential medium (MEM) α supplemented with 10% fetal bovine serum (FBS), 100 U/mL penicillin, 100 mg/mL streptomycin, and MEM vitamins solution. Cells were maintained at 37 $^{\circ}$ C in a humidified atmosphere of 5% CO₂. Cells (5×10^6 cells/condition) were seeded in 10% FBS medium for 12 h prior to the incubation (8 h) with test compound, or vehicle, in 1% FBS medium. Cells and medium were then recovered and the lipids extracted in the presence of deuterated 2-AG (200 pmol) by adding chloroform (14 mL) and methanol (5 mL). Following vigorous mixing and sonication, the samples were centrifuged and the organic layer was recovered and then dried under a stream of nitrogen. The resulting lipid extracts were purified by solid-phase extraction using silica and elution with an ethyl acetate–acetone (1:1) solution.³⁷ The resulting lipid fraction was analyzed by HPLC–MS using an LTQ-Orbitrap mass spectrometer (ThermoFisher Scientific) coupled to an Accela HPLC system (ThermoFisher Scientific).¹⁴ Analyte separation was achieved using a C-18 Supelguard precolumn and a Supelcosil LC-18 column (3 μ m, 4 mm \times 150 mm) (Sigma-Aldrich). Mobile phases A and B were composed of MeOH–H₂O–acetic acid, 75:25:0.1 (v/v/v) and MeOH–acetic acid 100:0.1 (v/v), respectively. The gradient (0.5 mL/min) was designed as follows: transition from 100% A to 100% B linearly over 15 min, followed by 10 min at 100% B and subsequent re-equilibration at 100% A. We performed MS analysis in the positive mode with an APCI ionization source. The capillary and APCI vaporizer temperatures were set at 250 and 400 $^{\circ}$ C, respectively.³⁸ 2-Arachidonoylglycerol was quantified by isotope dilution using 2-AG-*d*₅ standard showing identical retention time. The calibration curves were generated as described and the data normalized to vehicle-treated cells.³⁷

■ ASSOCIATED CONTENT

■ Supporting Information

Synthesis protocols of isothiocyanate, 2-bromo-1-phenylethanolone, and dithiocarbamate acid salt derivatives and analytical data for compounds 02, 04, 06–15, and 17–36. This material is available free of charge via the Internet at <http://pubs.acs.org>.

■ AUTHOR INFORMATION

Corresponding Author

*Phone: +32-2-764-7347. Fax: +32-2-764-7363. E-mail: didier.lambert@uclouvain.be.

Notes

The authors declare no competing financial interest.

■ ACKNOWLEDGMENTS

This work was supported by a research grant from the FNRS (FRSM Grant 3.4.625.07 and FRFC Grant 2.4.654.06). C.N.K. is very indebted to the “Fonds Spécial de Recherche” (Université Catholique de Louvain, Belgium) for his fellowships. The authors are also grateful to the Université Catholique de Louvain for a subsidy from the Fonds Speciaux de Recherches (FSR) and to the FNRS for a FRFC grant (FRFC Grant 2.4555.08).

■ ABBREVIATIONS USED

MAGL, monoacylglycerol lipase; 2-AG, 2-arachidonoylglycerol; ECS, endocannabinoid system; CB₁, cannabinoid subtype 1; CB₂, cannabinoid subtype 2; FAAH, fatty acid amide hydrolase; 2-OG, 2-oleoylglycerol; ABHD6, α/β hydrolase domain 6; ABHD12, α/β hydrolase domain 12; AEA, arachidonylethanolamine; WT, wild-type; DTT, dithiothreitol; THF, tetrahydrofuran

■ REFERENCES

- (1) Di Marzo, V. Endocannabinoids: Synthesis and Degradation. *Rev. Physiol. Biochem. Pharmacol.* **2008**, *160*, 1–24.
- (2) Kreitzer, A. C.; Regehr, W. G. Cerebellar Depolarization-Induced Suppression of Inhibition Is Mediated by Endogenous Cannabinoids. *J. Neurosci.* **2001**, *21* (RC174), 1–5.
- (3) Kishimoto, S.; Kobayashi, Y.; Oka, S.; Gokoh, M.; Waku, K.; Sugiura, T. 2-Arachidonoylglycerol, an Endogenous Cannabinoid Receptor Ligand, Induces Accelerated Production of Chemokines in HL-60 Cells. *J. Biochem.* **2004**, *135*, 517–524.
- (4) Gonsiorek, W.; Lunn, C.; Fan, X.; Narula, S.; Lundell, D.; Hipkin, R. W. Endocannabinoid 2-Arachidonoylglycerol Is a Full Agonist through Human Type 2 Cannabinoid Receptor: Antagonism by Anandamide. *Mol. Pharmacol.* **2000**, *57*, 1045–1050.
- (5) Savinainen, J. R.; Jarvinen, T.; Laine, K.; Laitinen, J. T. Despite Substantial Degradation, 2-Arachidonoylglycerol Is Potent Full Efficacy Agonist Mediating CB₁ Receptor-Dependent G-Protein Activation in Rat Cerebellar Membranes. *Br. J. Pharmacol.* **2001**, *134*, 664–672.
- (6) Stella, N.; Piomelli, D. Receptor-Dependent Formation of Endogenous Cannabinoids in Cortical Neurons. *Eur. J. Pharmacol.* **2001**, *425*, 189–196.
- (7) Ahn, K.; MacKinney, M. K.; Cravatt, B. F. Enzymatic Pathways That Regulate Endocannabinoid Signaling in the Nervous System. *Chem. Rev.* **2008**, *108*, 1687–1707.
- (8) Labar, G.; Michaux, C. Fatty Acid Amide Hydrolase: From Characterization to Therapeutics. *Chem. Biodiversity* **2007**, *4*, 1882–1902.
- (9) Deutsch, D. G.; Chin, S. A. Enzymatic Synthesis and Degradation of Anandamide, a Cannabinoid Receptor Agonist. *Biochem. Pharmacol.* **1993**, *46*, 791–796.

- (10) Marrs, W. R.; Blankman, J. L.; Horne, E. A.; Thomazeu, A.; Lin, Y. H.; Coy, J.; Bodor, A. L.; Muccioli, G. G.; Hu, S. S.; Woodruff, G.; Fung, S.; Lafourcade, M.; Alexander, J. P.; Long, J. Z.; Li, W.; Xu, C.; Möller, T.; Mackie, K.; Manzoni, O. J.; Cravatt, B. F.; Stella, N. The Serine Hydrolase ABHD6 Controls the Accumulation and Efficacy of 2-AG at Cannabinoid Receptors. *Nat. Neurosci.* **2010**, *13*, 951–957.
- (11) Dinh, T. P.; Kathuria, S.; Piomelli, D. RNA Interference Suggests a Primary Role for Monoacylglycerol Lipase in the Degradation of the Endocannabinoid 2-Arachidonoylglycerol. *Mol. Pharmacol.* **2004**, *66*, 1260–1264.
- (12) Blankman, J. L.; Simon, G. M.; Cravatt, B. F. A Comprehensive Profile of Brain Enzymes That Hydrolyze the Endocannabinoid 2-Arachidonoylglycerol. *Chem. Biol.* **2007**, *14*, 1347–1356.
- (13) Muccioli, G. G.; Xu, C.; Odah, E.; Cudaback, E.; Cisneros, J. A.; Lambert, D. M.; Rodriguez, M. L. L.; Bajjalieh, S.; Stella, N. Identification of a Novel Endocannabinoid-Hydrolyzing Enzyme Expressed by Microglial Cells. *J. Neurosci.* **2007**, *27*, 2883–2889.
- (14) Alhouayek, M.; Lambert, D. M.; Delzenne, N. M.; Cani, P. D.; Muccioli, G. G. Increasing Endogenous 2-Arachidonoylglycerol Levels Counteracts Colitis and Related Systemic Inflammation. *FASEB J.* **2011**, *25*, 2711–2721.
- (15) Nomura, D. K.; Long, J. Z.; Niessen, S.; Hoover, H. S.; Shu-Wing, N.; Cravatt, B. F. Monoacylglycerol Lipase Regulates a Fatty Acid Network That Promotes Cancer Pathogenesis. *Cell* **2010**, *140*, 49–61.
- (16) Nomura, D. K.; Lombardi, D. P.; Chang, J. W.; Niessen, S.; Ward, A. M.; Long, J. Z.; Hoover, H. H.; Cravatt, B. F. Monoacylglycerol Lipase Exerts Dual Control over Endocannabinoid and Fatty Acid Pathways To Support Prostate Cancer. *Chem. Biol.* **2011**, *18*, 846–856.
- (17) Labar, G.; Bauvois, C.; Borel, F.; Ferrer, J. L.; Wouters, J.; Lambert, D. M. Crystal Structure of the Human Monoacylglycerol Lipase, a Key Actor in Endocannabinoid Signaling. *ChemBioChem* **2010**, *11*, 218–227.
- (18) Bertrand, T.; Augé, F.; Houtmann, J.; Rak, A.; Vallée, F.; Mikol, V.; Berne, P. F.; Michot, N.; Cheuret, D.; Hoonart, C.; Mathieu, M. Structural Basis for Human Monoglyceride Lipase Inhibition. *J. Mol. Biol.* **2010**, *396*, 663–673.
- (19) Viso, A.; Cisneros, J. A.; Ortega-Gutierrez, S. The Medicinal Chemistry of Agents Targeting Monoacylglycerol Lipase. *Curr. Top. Med. Chem.* **2008**, *8*, 231–246.
- (20) Vandevoorde, S. Overview of the Chemical Families of Fatty Acid Amide Hydrolase and Monoacylglycerol Lipase Inhibitors. *Curr. Top. Med. Chem.* **2008**, *8*, 247–267.
- (21) Labar, G.; Bauvois, C.; Muccioli, G. G.; Wouters, J.; Lambert, D. M. Disulfiram Is an Inhibitor of Human Purified Monoacylglycerol Lipase, the Enzyme Regulating 2-Arachidonoylglycerol Signalling. *ChemBioChem* **2007**, *8*, 1293–1297.
- (22) Kapanda, C. N.; Muccioli, G. G.; Labar, G.; Poupaert, J. H.; Lambert, D. M. Bis(dialkylaminethiocarbonyl)disulfides as Potent and Selective Monoglyceride Lipase Inhibitors. *J. Med. Chem.* **2009**, *52*, 7310–7314.
- (23) Muccioli, G. G.; Labar, G.; Lambert, D. M. CAY10499, a Novel Monoglyceride Lipase Inhibitor Evidenced by an Expedient MGL Assay. *ChemBioChem* **2008**, *9*, 2704–2710.
- (24) Long, J. Z.; Li, W.; Booker, L.; Burston, J. J.; Kinsey, S. G.; Schlosburg, J. E.; Pavon, F. J.; Serrano, A. M.; Selley, D. E.; Parsons, L. H.; Lichtman, A. H.; Cravatt, B. F. Selective Blockade of 2-Arachidonoylglycerol Hydrolysis Produces Cannabinoid Behavioural Effects. *Nat. Chem. Biol.* **2009**, *5*, 37–44.
- (25) Kapanda, C. N.; Muccioli, G. G.; Labar, G.; Draoui, N.; Lambert, D. M.; Poupaert, J. H. Search for Monoglyceride Lipase Inhibitors: Synthesis and Screening of Arylthioamides Derivatives. *Med. Chem. Res.* **2009**, *18*, 243–254.
- (26) Munch, H.; Hansen, J. S.; Pittelkow, M.; Christensen, J. B.; Boas, H. A New Efficient Synthesis of Isothiocyanates from Amines Using Di-*tert*-butyl Dicarboxylate. *Tetrahedron Lett.* **2008**, *49*, 3117–3119.
- (27) Asinger, F.; Saus, A.; Offermans, H.; Heinz, D. Synthesis of oxothioamides and substituted 3-imidazoline-5-thiones. *Justus Liebigs Ann. Chem.* **1966**, *691*, 92–108.
- (28) Sekhar, N. M.; Acharyulu, P. V. R.; Anjaneyulu, Y. A short and efficient synthetic protocol for the synthesis of 5-substituted-4,6-dioxopyrrolo[2,3-*d*]pyrimidines. *Tetrahedron Lett.* **2011**, *52*, 4140–4144.
- (29) Liu, Y.; Bao, W. A new method for the synthesis of dithiocarbamates by CuI-catalyzed coupling reaction. *Tetrahedron Lett.* **2007**, *48*, 4785–4788.
- (30) Sattigeri, V. J.; Soni, A.; Singhal, S.; Khan, S.; Pandya, M.; Bhateja, P.; Mathur, T.; Rattan, A.; Khanna, J. M.; Mehtaa, A. Synthesis and antimicrobial activity of novel thiazolidinones. *ARKIVOC* **2005**, No. ii, 46–59.
- (31) Peterson, Q. P.; Hsu, D. C.; Goode, D. R.; Novotny, C. J.; Totten, R. K.; Hergenrother, P. J. Procaspase-3 Activation as an Anti-Cancer Strategy: Structure–Activity Relationship of Procaspase-Activating Compound 1 (PAC-1) and Its Cellular Co-Localization with Caspase-3. *J. Med. Chem.* **2009**, *52*, 5721–5731.
- (32) Labar, G.; Vliet, F. V.; Wouters, J.; Lambert, D. M. A MBP-FAAH Fusion Protein as a Tool To Produce Human and Rat Fatty Acid Amide Hydrolase: Expression and Pharmacological Comparison. *Amino Acids* **2008**, *34*, 127–133.
- (33) Bissantz, C.; Kuhn, B.; Stahl, M. A Medicinal Chemist's Guide to Molecular Interactions. *J. Med. Chem.* **2010**, *53*, 5061–5084.
- (34) King, A. R.; Lodola, A.; Carmi, C.; Fu, J.; Mor, M.; Piomelli, D. A Critical Cysteine Residue in Monoacylglycerol Lipase Is Targeted by a New Class of Isothiazolinone-Based Enzyme Inhibitors. *Br. J. Pharmacol.* **2009**, *157*, 974–983.
- (35) Long, J. Z.; Jin, X.; Adibekian, A.; Li, W.; Cravatt, B. F. Characterization of Tunable Piperidine and Piperazine Carbamates as Inhibitors of Endocannabinoid Hydrolases. *J. Med. Chem.* **2010**, *53*, 1830–1842.
- (36) Ahn, K.; Johnson, D. S.; Fitzgerald, L. R.; Liimatta, M.; Arendse, A.; Stevenson, T.; Lund, E. T.; Nugent, R. A.; Nomanbhoy, T. K.; Alexander, J. P.; Cravatt, B. F. Novel Mechanistic Class of Fatty Acid Amid Hydrolase Inhibitors with Remarkable Selectivity. *Biochemistry* **2007**, *46* (45), 13019–13030.
- (37) Muccioli, G. G.; Stella, N. An Optimized GC–MS Method Detects Nanomolar Amounts of Anandamide in Mouse Brain. *Anal. Biochem.* **2008**, *373*, 220–228.
- (38) Muccioli, G. G.; Naslain, D.; Backhed, F.; Reigstad, C. S.; Lambert, D. M.; Delzenne, N. M.; Cani, P. D. The Endocannabinoid System Links Gut Microbiota to Adipogenesis. *Mol. Syst. Biol.* **2010**, *6*, 392.